ELSEVIER

14 August 2000

Physics Letters A 273 (2000) 109–116

PHYSICS LETTERS A

www.elsevier.nl/locate/pla

Gravity induced granular flow measurements in a 2D silo with a lateral bottom exit

A. Medina [a,*], J. Andrade [b], J.A. Córdova [b], C. Treviño [b]

[a] *Subdirección de Exploración y Producción IMP, A.P. 14-805, 07730 Mexico D.F., Mexico*
[b] *Departamento de Fisica, Facultad de Ciencias, UNAM, A.P. 70-564, 04510 Mexico D.F., Mexico*

Received 12 June 2000; received in revised form 26 June 2000; accepted 7 July 2000
Communicated by A.R. Bishop

Abstract

Through the use of the particle image velocimetry (PIV) technique, we have measured and analyzed the gravity-driven granular flow in a flat bottomed 2D silo, with the exit hole located close to a vertical wall of the silo. The main properties of the unsteady flow like the intensity of the velocity fluctuations and the time averaged velocity field were determined. The global oscillations observed in a silo with the exit hole located at the center have not been detected in this case, being related to the larger mass flow rate obtained with the exit located far from the center. © 2000 Elsevier Science B.V. All rights reserved.

PACS: 46.10.+z; 05.40.+j
Keywords: Mechanics of discrete systems; Fluctuation phenomena

1. Introduction

The study of gravity-driven flow of dry, noncohesive granular material from silos or storage devices represents an important field of research. This is because of the related industrial applications and the large variety of the physical phenomena occurring like arching, size segregation, density waves, density fluctuations, transversal oscillations and transient flow processes [1–3]. All these phenomena are in essence due to the nature of granular matter. The central problem in these type of processes is the lack of governing equations for all flow properties, such as scalar fields like pressure and density and vectorial fields like velocity. The grains interact between them through inelastic shocks, grain's rotations and frictional contacts, producing very complex flow structures. The geometry of the silo is of fundamental importance, which has a large influence in the resulting flow patterns. We reported in a previous Letter, an experimental study of the whole transient velocity field in a near two-dimensional (2D) silo filled with equal-sized spherical grains (glass beads) with the exit hole located at the center of the bottom [4]. In that case strong global flow oscillations were detected, with an important momentum interchange from grains coming from both sides of the symmetry plane, producing a reduction of the mass flow rate of grains from the silo. Contrary to the symmetrical

* Corresponding author. Fax: +52 5 5 67 82 32.
E-mail address: amedina@www.imp.mx (A. Medina).

PII: S0375-9601(00)00473-4

case, the granular flow using a lateral exit, has been seldom studied, though it produces a 10–20% increase in the mass flow rate, with the same exit and silo dimensions [5–7]. The quantitative understanding of the increase of the mass flow rate in this flow still lacks a satisfactory theoretical background.

The objective of this Letter is the study of the flow structure using the same silo configuration reported previously [4], but using a lateral exit instead of the exit located at the symmetry plane (see Fig. 1). An interesting fact in this geometry, is that during the discharge of tall enough silos, the mass flow rate is larger compared with the silo with the exit located at the center (symmetrical configuration). Based on experiments, we did not detect the flow oscillations for the case of the exit hole located laterally (close to the vertical wall). Using this fact, we give an explanation for the increase of the mass flow rate for this geometry. As an attempt to bring strong foundations to the understanding of this flow, we have obtained here the whole velocity field and their properties, by considering the granular flow when the size of the bottom exit, D, was maintained constant. In particular, the initial transient and the full developed granular flow are studied in this work. In Section 2, we describe the experimental setup and the method employed to obtain the velocity field. In Section 3 we give an order of magnitude estimation of the evolution time of the initial transient flow. In Section 4 we obtained the velocity fluctuations and the mean velocity components at several heights. In this Section, we also discuss how these quantities provide new insights in the behavior of this complex flow. Finally, in Section 5 we give a discussion and a brief comparison with the symmetrical case, together with the main conclusions.

2. Experimental approach

In the past, optical methods like interference have been seldom used to detect detailed experimental particle displacements in granular media flow. Only few years ago, the speckle photography was introduced to obtain the 2D displacement field in a small zone of material and the quasi-rigid behavior during the slow penetration of solids in granular media [8]. Recently, we have employed the particle image velocimetry (PIV) technique [4], based on similar principles that those for speckle photography (Young's

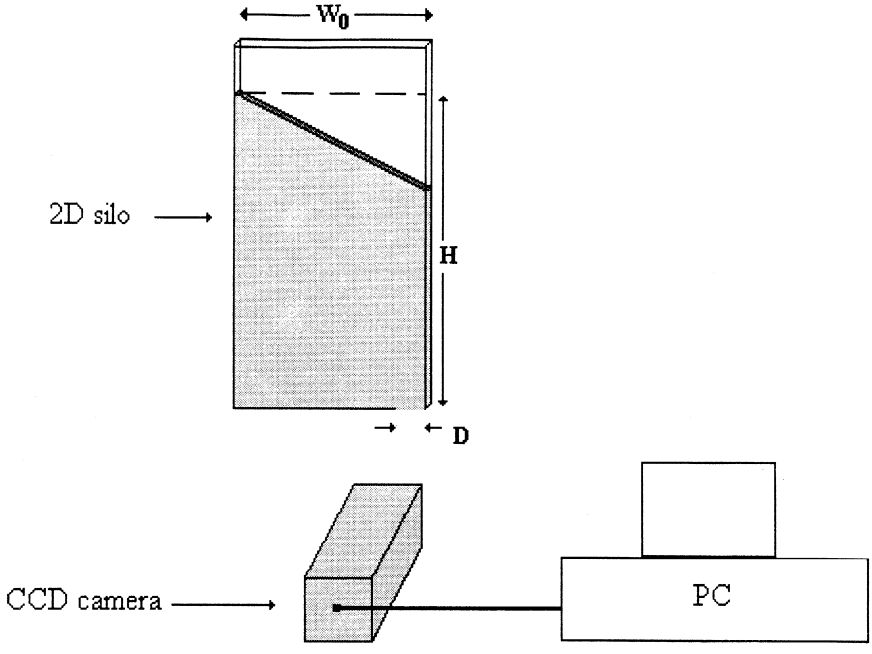

Fig. 1. Experimental setup and geometrical parameters of the flat-bottomed silo with lateral aperture.

fringe patterns of the double exposed speckle or particle images), to measure the velocity field in the granular flow within a 2D silo. For this type of granular flows, a very good resolution for the velocity field for a long time and in a widely extended spatial zone, has been obtained.

The flow has been induced by gravity in a vertical glass-walled silo of 100 cm height, $W_0 = 30.0$ cm width and 3.8 mm deep filled up to $H = 90$ cm with monodisperse granular material composed of spherical glass-beads with mean diameter $d = 3.15 \pm 0.04$ mm, mean friction static coefficient $\mu = 0.57$ and grain density $\rho_p = 2.45$ gr/cm^3 (see Fig. 1). The upper part of the silo is open to ambient pressure, so we can neglect the influence of air bubbles going up in closed silos, which is typical in the classical hourglasses. The flow with no overlapping grains, passing through a lateral aperture $D = 2$ cm size, was recorded with a fast-shutter-speed (1/500 s) CCD camera with a video rate of 30 frames per second (30 Hz). The velocity field measurements in the 2D silo were made in three different phases: (a) Flow recording, (b) digitization and (c) PIV analysis. In the second phase (b), each recorded frame has been fed into a computer and digitized as a digital image with a 256-gray scale. Finally, in phase (c) we used the PIV analysis software to obtain the grain displacements between two consecutive frames. By employing this technique, the displacements of a small group of grains can be determined. The images are divided in a mesh of interrogation regions. The measurements are obtained for each interrogation region, using two consecutive digitized images with an elapsed time between them. The vectorial displacements $\Delta \boldsymbol{x}$ of particles within this region are determined through the two-frame cross-correlation. Here, both images are correlated to each other and the velocity vector $\boldsymbol{v}$ in the plane of flow is obtained at each position in the flow field as $\boldsymbol{v} = M\Delta \boldsymbol{x}(\boldsymbol{r})/\Delta t$, where M is the image magnification factor, $\Delta t = 1/30$ s is the time interval between images (frames), and $\boldsymbol{r} = (x', y')$ refers to the centroid position of the interrogation region.

For each consecutive pair of frames, we obtained a local space-averaged velocity vector $\boldsymbol{v} = (u(t), v(t))$, at a fixed position (the center of the interrogation area). Therefore, with this technique we can obtain the whole velocity field in the region covered by the image. The measurement region of the granular flow has a size of 30 cm height by 20 cm width. The number of interrogation areas along the x (transverse) and y (longitudinal) directions must be large enough to obtain a good resolution of the velocity field. The PIV software produces data files containing $N = 30$ velocity vectors at a given height, y. The number of different heights was $L = 20$, so we have $N \times L$ (in our case 600) velocity vectors in the measurement region at each time. Finally, we obtained 360 frames, which represents 12 s of the granular flow. This is enough to resolve from .05 to 15 Hz in this transient process. Under these conditions, the errors primarily result from the uncertainty in determining the centroids of the particles, producing in our case errors in the velocities around 1%. A more detailed description of this technique for the case of a 2D symmetrical case, can be found elsewhere [4]. In this work we have chosen between 10 and 50 of the overlapping interrogation areas along each direction, without obtaining important differences in all quantities derived from the velocity vectors.

3. Initial transient flow

The velocity vectors for the initial transient process at different times after opening the exit port are shown in Fig. 2. For this particular case, we obtained the whole velocity field using 600 velocity vectors (30 vectors along the x-axis and 20 vectors along the y-axis). At the time of the initiation of discharge, that is as the exit hole is opened, the flow field establishes within a region whose boundary propagates with time both upward and toward the opposite silo wall, as shown in Fig. 2. Above that boundary, the grains are closely packed and they mutually impede each other to move. Below the boundary, the grains are loose packed and few frictional contacts occur so the grains move with a certain acceleration under the influence of gravity. Qualitative aspects of the transient initial flow have been already analyzed (see for instance Ref. [9]). We will estimate the order of magnitude for the density wave propagation in this inertial dominated phenomenon. The order of magnitude of the velocity of the grains at the exit port of the silo, assuming a large ratio of the exit

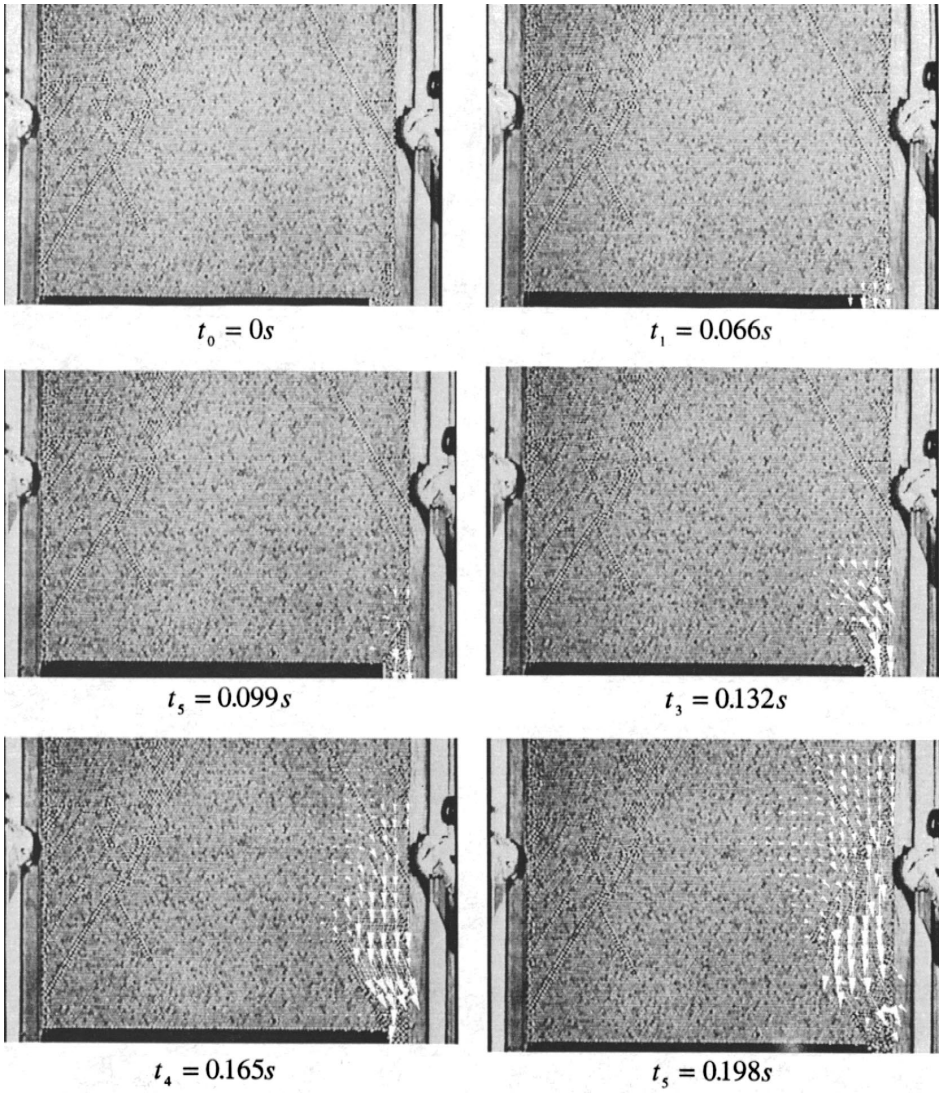

Fig. 2. Initial velocity fields for the flow in a 2D silo using a lateral exit port, with the granular material being visualized. We show snapshots with their corresponding times, of the transient velocity field during the first 0.12 s after the aperture of the exit port.

port size D to the particle diameter ϕ, is using dimensional arguments $v_E \sim \sqrt{gD}$, while the characteristic velocity far above the exit using mass conservation, must be of the order $v \sim \sqrt{gD^3}/W$, where W is the width of the of the flow zone, which is a function of the height y, given by $W/D = (y/y_0 + 1)$. Fig. 3 shows the characteristic lengths where y_0 is the distance from the imaginary flow vertex (denoted by 0) to the bottom exit port. This point is to be determined by the dynamic angle of approach θ, during the flow. At the density wave front, the grains reach the assumed velocity for fully developed flow under the influence of gravity acceleration g, in accordance with the relation $v \sim gt_c \sim \sqrt{gD^3}/W$, where t_c is the characteristic time needed for the particle to reach such velocity. The order of magnitude of the characteristic time, which depends on the height is then $t_c \sim D^{3/2}W^{-1}g^{-1/2}$. Due to the fact that the grain size is very small compared with the silo size, we can transform the above relationships to

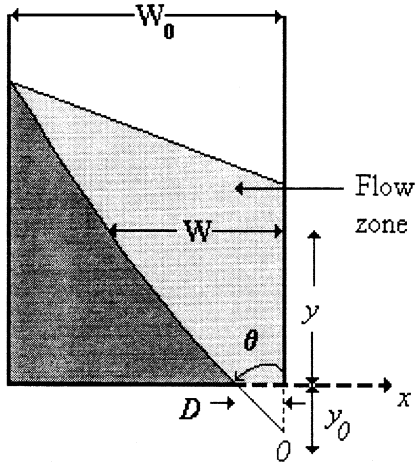

Fig. 3. Schematic view of the geometrical parameters of the silo considered for the transient initial process.

a first order differential equation for the propagation of the density front. Using the nondimensional variables $\eta = y/y_0$ and $\tau = \phi\sqrt{g/D}\,t/y_0$, the nondimensional equation (neglecting the effect of friction) for a grain which is affected by the motion at the border of the density wave front is given by $d\eta/d\tau = 1 + \eta$. Therefore, the solution to this equation is $\tau = \ln(\eta + 1)$. By using this last relationship, we can determine the time for the flow to be well developed within our measurement zone ($y = 20$ cm). Visually, we obtain from Fig. 3 a time $t \sim 0.2$ s, while the estimation taking into account that $\theta \simeq 32.5°$, $y_0 \sim 3.4$ cm, $\phi \sim 0.3$ cm and $D \sim 2$ cm, gives from $t \sim 0.8$ s.

4. Fully developed flow field

In this section we analyze the fully developed unsteady flow and its mean properties. One important aspect in the knowledge of the developed flow is the evaluation of the velocity field fluctuations from the respective averaged values. We will split the non-steady velocity field of particles $\boldsymbol{v}$ into the mean and its fluctuating quantity, that is $\boldsymbol{v} = \langle \boldsymbol{v} \rangle + \boldsymbol{v}'$, with $\langle \boldsymbol{v}' \rangle = 0$. We have computed the time-averaged velocity components $\langle u \rangle$ in the transverse direction and $\langle v \rangle$ in the longitudinal direction, using the data obtained for 12 s, normalized both with $\sqrt{gD}$, which is representative of the velocity at the exit. These profiles are shown in Fig. 4 at three dimensionless heights in the silo. In Fig. 4a we show the profiles of the mean horizontal component while in Fig. 4b the profiles of the mean vertical component are shown. The behavior in this case is different to that reported for the symmetrical configuration [4] where the experimental data showed a very good agreement with the kinematic model [1]. Here, both velocity profiles were fitted by the curves

$$\langle \underline{v} \rangle = -\langle \underline{v}_0 \rangle \exp\left[-\frac{(\underline{x} - \underline{x}_{cy})^2}{4B\underline{y}} \right], \tag{1}$$

and

$$\langle \underline{u} \rangle = \langle \underline{u}_0 \rangle \exp\left[-\frac{(\underline{x} - \underline{x}_{cx})^2}{4C\underline{y}} \right], \tag{2}$$

where $\langle \underline{v} \rangle$ and $\langle \underline{u} \rangle$ are the normalized mean, vertical and horizontal averaged velocity profiles, respectively. Similarly, $\underline{x}$, $\underline{y}$, B and C are all normalized by W_0. The quantities $\langle \underline{v}_0 \rangle$ and $\langle \underline{u}_0 \rangle$ are the maxima of the corresponding velocity profiles which are reached respectively just at the point $\underline{x} = \underline{x}_{cy}$ and $\underline{x} = \underline{x}_{cx}$,i.e., the maximum velocities are reached in points close to the right wall of the silo. These points obey the correlations

$$\underline{x}_{cy} = -0.07\underline{y} + 0.93 \text{ and } \underline{x}_{cx} = -0.11\underline{y} + 0.90. \tag{3}$$

These last correlations show that, at the bottom ($\underline{y} = 0$), the mean vertical velocity component has its maximum just at the center of the exit and the horizontal velocity has the maximum not at the center but close to it. This last fact may be due to the rebound of the grains on the wall. The kinematic parameter B changes with the dimensionless height in a non-linear form while the kinematic parameter C is approximately constant with height

$$B \simeq 0.0038e^{0.42\underline{y}} \text{ and } C \simeq 0.005. \tag{4}$$

The intensity of the velocity fluctuations is given by the root mean square (rms) of the fluctuating part of the velocity field normalized with the mean velocity, which are represented by

$$(Tu, Tv) = \left(\frac{\langle u'u' \rangle^{1/2}}{\langle u \rangle}, \frac{\langle v'v' \rangle^{1/2}}{\langle v \rangle} \right), \tag{5}$$

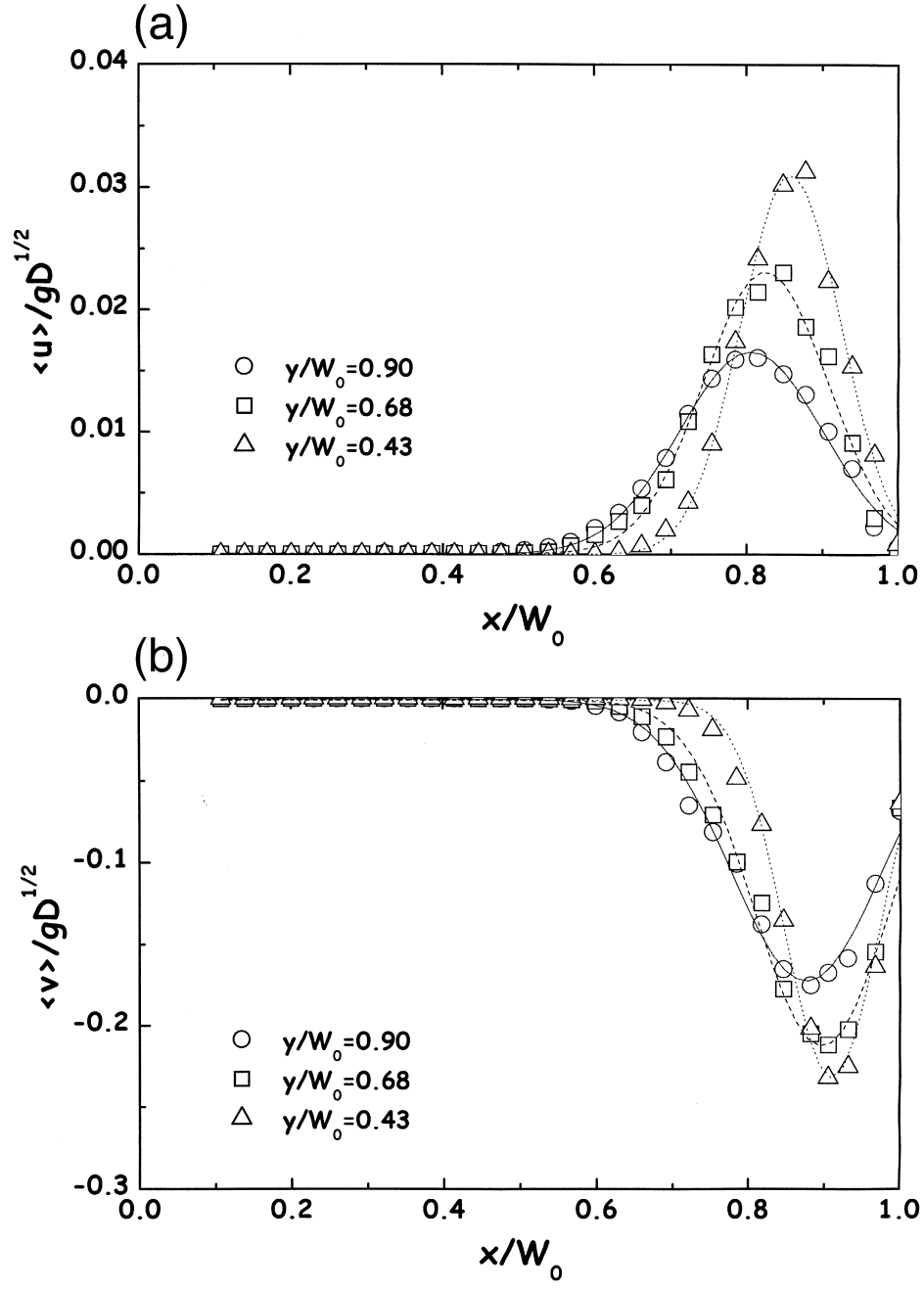

Fig. 4. Dimensionless, time-averaged velocity profiles at three different dimensionless heights. In (a) we show the nondimensional mean transverse velocity profiles and their fit (curves) while in (b) we show the same for the vertical velocity component. The time averaging was made for a period of 12 s.

where u' and v' are the components of the fluctuating part, $\boldsymbol{v}'$, of the non-steady velocity field. In Fig. 5 we show the plot of Tu (Fig. 5a) and Tv (Fig. 5b) as a function of $\underline{x} = x/W_0$ for three different dimen-

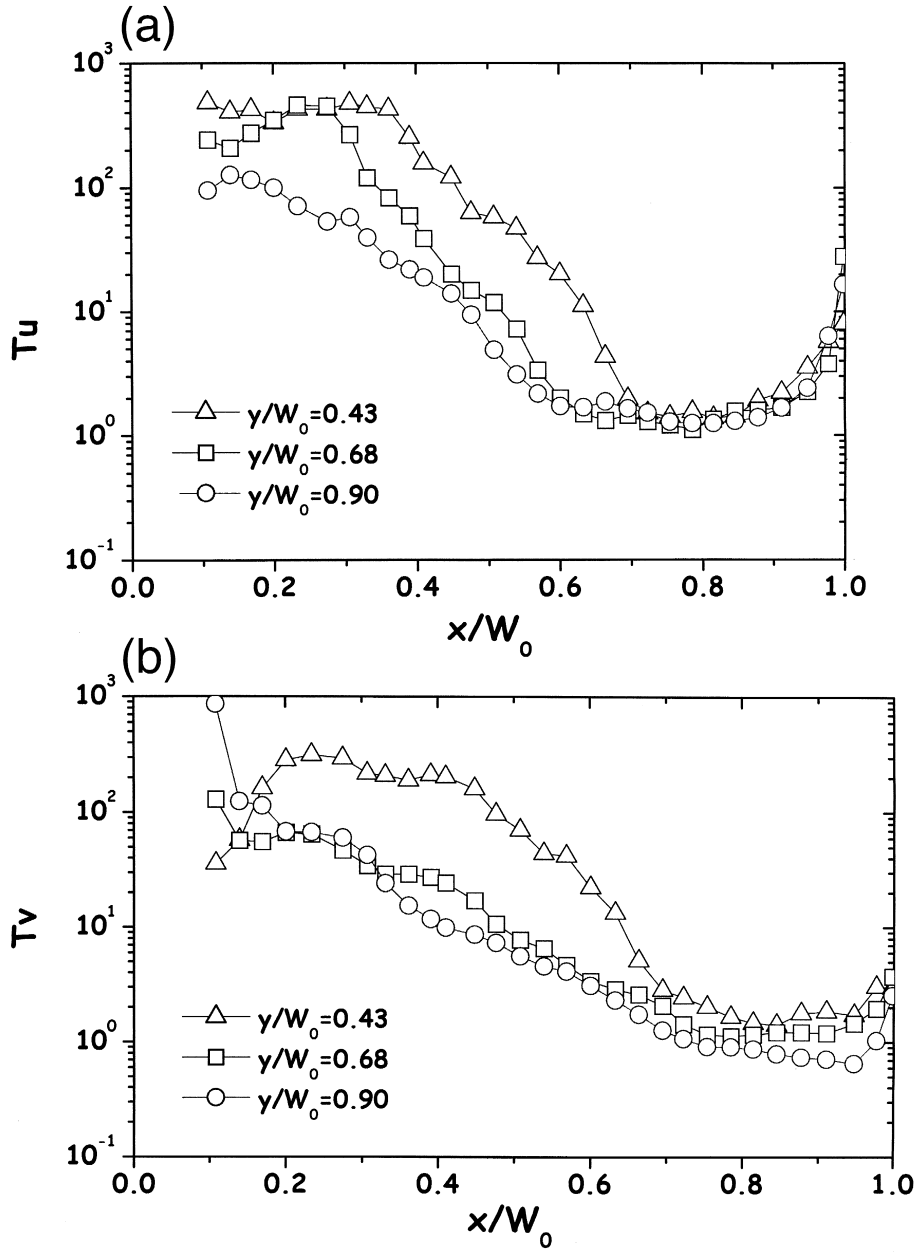

Fig. 5. Root mean square of the velocity fluctuations, normalized with the mean velocity at three different dimensionless heights. (a) corresponds to the transversal component while (b) corresponds to the vertical component.

sionless heights, measured from the bottom, $y/W_0 = 0.48$, 0.63, and 0.90. These patterns are typical of this flow and their forms correspond qualitatively to the left-hand-side of those of the symmetrical case. We notice however, that the intensity of the fluctuations for the rms of $u(t)$, is one order of magnitude larger than in the symmetrical case. We think that this fact is a measure of the loose packing along the transversal direction and consequently the component of friction along this direction is lower.

In order to study the unsteady structures detected in the velocity field, we search for characteristic transversal oscillations, which have been observed in the symmetrical configuration [4]. We employ the same methodology used in the previous work by the authors [4], to show the lack of any global characteristic frequency in the fully developed flow. Briefly, the evaluation of the power spectrum was based on the construction of the variable $G(t)$, which gives the time dependency of the centroid generated by the longitudinal velocity component, defined by

$$G(t) = X - \langle X \rangle, \tag{6}$$

where

$$X = \frac{1}{N\bar{v}} \sum_{i=1}^{N} x_i v_i, \tag{7}$$

and N, as aforementioned, corresponds to the number ($N = 30$) of data points i at a given height, y, and x_i is the value of x at node i measured from the left wall of the silo. The quantity $\bar{v}(t) = \left(\sum_{i=1}^{N} v_i\right)/N$, denotes the spatial averaged vertical velocity at a given height, while $\langle\ \rangle$ denotes a time averaged quantity. From the definition of $G(t)$, then $\langle G(t) \rangle = 0$. Contrary as obtained for the symmetrical case, we could not find any important characteristic frequency from the power spectrum of the autocorrelation function of $G(t)$. Clearly, the asymmetry of the configuration is the main cause for the elimination of transversal oscillations, which are present in the symmetrical configuration.

5. Conclusions

The main objective of this work is to show the influence of the position of the exit port of a 2D silo using the same silo configuration reported previously [4], but with the exit position located laterally. The non-intrusive technique of measurement called Particle Image Velocimetry has been used to study experimentally the mean and the unsteady granular velocity field in a wide spatial zone for a relatively long time. In the experiments we analyzed a total of 360 frames, covering around 12 seconds at 30 frames per second. We obtained both qualitative as well as quantitative information on the flow structure. In this sense, we could resolve velocity fluctuations from 0.083 to 15 Hz. In typical experiments we obtained around 600 instantaneous velocity vector plots, covering the whole area at the bottom of the silo. The white noise associated with the power spectrum of $G(t)$, indicates the lack of any characteristic frequency. Using this configuration we could not detect global oscillations of the flow as previously reported for the symmetric case. These oscillations are one of the main factor which produces an important reduction of the mass flow rate. We also have obtained the mean velocity and the fluctuation intensities, given by the normalized root mean square of the fluctuating velocity of particles. We notice an increase in the intensity of fluctuations, compared with the symmetrical flow, for the transversal component of the velocity field. Finally, the mean velocity field was obtained but the kinematic model does not give a good agreement with the experimental velocity profiles, ($\langle \underline{u} \rangle$,$\langle \underline{v} \rangle$). The main change in this case is that, in the kinematic model, the horizontal averaged velocity has the form $\langle \underline{u} \rangle = -B\partial\langle \underline{v} \rangle/\partial \underline{x}$, while in the experiments it does not occur. More efforts in order to understand this last fact are in progress.

Acknowledgements

We acknowledge Prof. E. Ramos and his Group, for the support in using digitization software and equipment. We also acknowledge E. Luna his aid in use of PIV software.

References

[1] R.M. Nedderman, Statics and Kinematics of Granular Media, Cambridge University Press, Cambridge, England, 1992.
[2] B.J. Ennis, J. Green, R. Davies, Chem. Engin. Prog. 32 (1994) 32.
[3] T.M. Knowlton, J.W. Carlson, G.E. Klinzing, W.-C. Yang, Chem. Engin. Prog. 32 (1994) 44.
[4] A. Medina, A. Cordova, E. Luna, C. Treviño, Phys. Lett. A 250 (1999) 111.
[5] I.I. Kotchanova, Powder Technol. 4 (1970) 32.
[6] U. Tuzun, G.T. Houlby, R.M. Nedderman, S.B. Savage, Chem. Engin. Sci. 37 (1982) 1597.
[7] K. Wieghardt, Ann. Rev. Fluid. Mech. 7 (1975) 89.
[8] M. Monti, Speckle photography applied to the detailed study of the mechanical behavior of granular media, in: J. Biarez, R. Gourvez (Eds.), Powders and Grains, A.A. Balkema, Rotterdam, 1989, pp. 83–89.
[9] P. Arteaga, U. Tuzun, Chem. Engin. Sci. 45 (1990) 205.